

Probing the QCD equation of state with thermal photons in nucleus-nucleus collisions at RHIC

David d'Enterria ^a, Dmitri Peressounko ^b

^a*Nevis Laboratories, Columbia University,
Irvington, NY 10533, and New York, NY 10027, USA*

^b*RRC "Kurchatov Institute", Kurchatov Sq. 1, Moscow, 123182, Russia*

Abstract

Thermal photon production at mid-rapidity in Au+Au reactions at $\sqrt{s_{NN}} = 200$ GeV is studied in the framework of a hydrodynamical model that describes efficiently the bulk identified hadron spectra at RHIC. The combined thermal plus perturbative photon spectrum is in good agreement with the yields measured by the PHENIX experiment for all Au+Au centralities. Within our model, the correlation of the thermal photon slopes with the charged hadron multiplicity in each centrality bin provides direct empirical information on the underlying degrees of freedom and on the equation of state of the radiating matter.

PACS: 12.38.Mh, 24.10.Nz, 25.75.-q, 25.75.Nq

1 Introduction

Numerical calculations of lattice QCD predict a transition from ordinary hadronic matter to a deconfined state of quarks and gluons when the temperature of the system is of the order of $T_{crit} \approx 0.17$ GeV [1]. The existence of such a phase transition manifests itself clearly in the QCD equation-of-state (EoS) on the lattice by a sharp jump of the (Stefan-Boltzmann) scaled energy density, $\varepsilon(T)/T^4$, at the critical temperature, reminiscent of a first-order phase change¹. The search for evidences of this deconfined plasma of quarks and gluons (QGP) is the main driving force behind the study of relativistic nuclear

¹ The order of the phase transition itself is not exactly known: the pure SU(3) gauge theory is first-order whereas introduction of 2+1 flavours makes it of a fast cross-over type [1].

collisions at different experimental facilities in the last 20 years. Whereas several experimental results have been found consistent with the formation of the QGP both at CERN-SPS [2] and BNL-RHIC [3] energies, it is fair to acknowledge that there is no incontrovertible proof yet of bulk deconfinement in the present nucleus-nucleus data. In this letter, we present a detailed study of the only experimental signature, thermal photons, that can likely provide direct information on the *thermodynamical* properties (and, thus, on the equation-of-state) of the underlying QCD matter produced in high-energy heavy-ion collisions. Electromagnetic radiation (real and virtual photons) emitted in the course of a heavy-ion reaction, has long [4,5] been considered a privileged probe of the space-time evolution of the colliding system², inasmuch as photons are not distorted by final-state interactions due to their weak interaction with the surrounding medium. Direct photons, defined as real photons not originating from the decay of final hadrons, are emitted at various stages of the reaction with several contributing processes. Two generic mechanisms are usually considered: (i) *prompt* (pre-equilibrium or pQCD) photon emission from perturbative parton-parton scatterings in the first tenths of fm/c of the collision process, (ii) subsequent γ emission from the *thermalized* partonic (QGP) and hadronic (hadron resonance gas, HRG) phases of the reaction.

Experimentally, direct γ have been indeed measured in Pb+Pb collisions at CERN-SPS ($\sqrt{s_{NN}} = 17.3$ GeV) [9]. However, the relative contributions to the total spectrum of the pQCD, QGP and HRG components have not been determined conclusively. Different hydrodynamics calculations [10–14] require “non-conventional” conditions: high initial temperatures ($T_0^{max} > T_{crit}$), strong partonic and/or hadronic transverse velocity flows, or in-medium modifications of hadron masses, in order to reproduce the observed photon spectrum. However, no final conclusion can be drawn from these results due mainly to the uncertainties in the exact amount of radiation coming from primary parton-parton collisions. In a situation akin to that affecting the interpretation of high p_T hadron data at SPS [15], the absence of a concurrent baseline experimental measurement of prompt photon production in p+p collisions at the same \sqrt{s} and p_T range as the nucleus-nucleus data, makes it difficult to have any reliable empirical estimate of the actual thermal γ excess in the Pb+Pb spectrum. In the theoretical side, the situation at SPS is not fully under control either: (i) next-to-leading-order (NLO) perturbative calculations are known to under-predict the experimental reference nucleon-nucleon γ differential cross-sections below $\sqrt{s} \approx 30$ GeV [16] (a substantial amount of parton intrinsic transverse momentum k_T [17], approximating the effects of parton Fermi motion and soft gluon radiation, is required), (ii) the implementation of the extra nuclear k_T broadening observed in the nuclear data (“Cronin enhancement” [18] resulting from multiple soft and semi-hard interactions of the colliding partons on their

² Excellent reviews on photon production in relativistic nuclear collisions have been published recently [6–8].

way in/out the traversed nucleus) is model-dependent [19–21] and introduces an additional uncertainty to the computation of the yields, and (iii) hydrodynamical calculations usually assume initial conditions (longitudinal boost invariance, short thermalization times, zero baryochemical potential) too idealistic for SPS energies. The situation at RHIC (and LHC) collider energies is undoubtedly far more advantageous. Firstly, the photon spectra for different centralities in Au+Au [22] and in (baseline) p+p [23] collisions at $\sqrt{s} = 200$ GeV are already experimentally available. Secondly, the p+p baseline reference is well under control theoretically (NLO calculations do not require extra non-perturbative effects to reproduce the hard spectra at RHIC [23,24]). Thirdly, the amount of nuclear Cronin enhancement experimentally observed is very modest (high p_T π^0 are barely enhanced in d+Au collisions at $\sqrt{s_{NN}} = 200$ GeV [25]), and one expects even less enhancement for γ which, once produced, do not gain any extra k_T in their way out through the nucleus. Last but not least, the produced system at midrapidity in heavy-ion reactions at RHIC is much closer to the zero net baryon density and longitudinally boost-invariant conditions customarily presupposed in the determination of the parametrized photon rates and in the hydrodynamical calculations of the reaction evolution. In addition, the thermalization times usually assumed ($\tau_{therm} \lesssim 1$ fm/c) are, for the first time at RHIC, above the lower limit imposed by the transit time of the two colliding nuclei ($\tau_0 = 2R/\gamma = 0.15$ fm/c for Au+Au at 200 GeV). As a matter of fact, it is for the first time at RHIC that hydrodynamics predictions agree *quantitatively* with most of the differential observables of bulk (“soft”) hadronic production below $p_T \approx 1.5$ GeV/c in Au+Au reactions [26–28].

In this context, the purpose of this paper is three-fold. First of all, we present a relativistic 2D+1 hydrodynamics model that reproduces well the identified hadron spectra measured at all centralities in Au+Au collisions at $\sqrt{s_{NN}} = 200$ GeV. Secondly, using such a model complemented with the most up-to-date parametrizations of the QGP and HRG photon emission rates, we determine the expected thermal photon yields in Au+Au reactions and compare them to the prompt photon yields computed in NLO perturbative QCD. The combined inclusive (hydro+pQCD) photon spectrum is successfully confronted to very recent results from the PHENIX collaboration. Thirdly, after discussing in which p_T range the thermal photon signal can be potentially identified experimentally, we address the issue of how to have access to the thermodynamical properties (temperature, entropy) of the radiating matter. We propose the correlation of two experimentally measurable quantities: the thermal photon slope and the multiplicity of charged hadrons produced in the reaction, as a direct method to determine the underlying degrees of freedom and the equation of state of the dense and hot QCD medium produced in Au+Au collisions at RHIC energies.

2 Hydrodynamical model

Implementation. Hydrodynamical approaches of particle production in heavy-ion collisions assume *local* conservation of energy and momentum in the hot and dense strongly interacting matter produced in the course of the reaction and describe its evolution using the equations of motion of ideal (non-viscous) relativistic hydrodynamics. These equations are nothing but the conservation of: (i) the energy-momentum tensor: $\partial_\mu T^{\mu\nu} = 0$ with $T^{\mu\nu} = (\varepsilon + p)u^\mu u^\nu - p g^{\mu\nu}$ [where ε , p , and $u^\nu = (\gamma, \gamma v)$ are resp. the energy density, pressure, and collective flow 4-velocity fields, and $g^{\mu\nu} = \text{diag}(1, -1, -1, -1)$ the metric tensor], and (ii) the conserved currents in strong interactions: $\partial_\mu J_i^\mu = 0$, with $J_i^\mu = n_i u^\mu$ [where n_i is the number density of the net baryon, electric charge, net strangeness currents]. These equations complemented with three input ingredients: (i) the initial conditions (ε_0 at time τ_0), (ii) the equation-of-state of the system, $p(\varepsilon, n_i)$, relating the local thermodynamical quantities, and (ii) the freeze-out conditions, describing the transition from the hydrodynamics regime to the free streaming final particles, are able to reproduce most of the bulk hadronic observables measured in heavy-ion reactions at RHIC [26–28].

The particular hydrodynamics implementation used in this work is discussed in detail in [12]. As done in most of the works, we assume longitudinal boost-invariant (Bjorken) expansion [30] which reduces the equations of motion to a two-dimensional problem (2D+1 hydrodynamics), but results in a loss of the dependence of the observables on longitudinal degrees of freedom. Our results, thus, are only relevant for particle production within a finite range around midrapidity³. The equation-of-state used here describes a first order phase transition from a QGP to a HRG at $T_{crit} = 165$ MeV with latent heat⁴ $\Delta\varepsilon \approx 1.4$ GeV/fm³, very similar to that used in other works [26]. The QGP is modeled as an ideal gas of massless quarks ($N_f = 2.5$ flavours) and gluons with total degeneracy $g_{QGP} = (g_{gluons} + 7/8 g_{quarks}) = 42.25$. The corresponding EoS, $p = 1/3\varepsilon - 4/3B$ (B being the bag constant), has sound velocity $c_s^2 = \partial p / \partial \varepsilon = 1/3$. The hadronic phase is modeled as a non-interacting gas of ~ 400 known hadrons and hadronic resonances with masses below 2.5 GeV/ c^2 . The inclusion of heavy hadrons leads to an equation of state significantly different than that of an ideal gas of massless pions: the velocity of sound in the HRG phase is $c_s^2 \approx 0.15$, resulting in a relatively soft hadronic EoS as suggested by lattice calculations [29]; and the effective number of degrees of freedom at T_c is $g_{HRG} \approx$

³ The experimental π^\pm and K^\pm dN/dy distributions at RHIC are Gaussians [31], as expected from perturbative QCD initial conditions [32]. Although there is no Bjorken rapidity plateau, the widths of the distributions are quite broad and within $|y| \lesssim 2$, deviations from boost invariance are not very large [32].

⁴ Although the lattice results seem to indicate that the transition is of a fast cross-over type, the predicted change of $\Delta\varepsilon \approx 0.8$ GeV/fm³ in a narrow temperature interval of $\Delta T \approx 20$ MeV [1] can be interpreted as the latent heat of the transition.

12 (as given by $g_{\text{eff}} = 45 \text{ s}/(2\pi^2 T^3)$, see later). Both phases are connected via the standard Gibbs' condition of phase equilibrium, $p_{QGP}(T_c) = p_{HRG}(T_c)$, during the mixed phase. The external bag pressure, calculated to fulfill this condition at T_c , is $B \approx 0.38 \text{ GeV}/\text{fm}^3$.

Statistical model analyses of particle production in nucleus-nucleus reactions [33] provide a very good description of the measured particle ratios at RHIC, assuming that all hadrons are emitted from a thermalized system reaching chemical equilibrium at a temperature T_{chem} with baryonic, strange and isospin chemical potentials μ_i . In agreement with those observations, our specific hydrodynamical evolution reaches chemical freeze-out at $T_{\text{chem}} = 150 \text{ MeV}$, and has $\mu_B = 25 \text{ MeV}$, $\mu_S = \mu_I = 0$. For temperatures above T_{chem} we conserve baryonic, strange and charge currents, but not particle numbers, while for temperatures below T_{chem} we explicitly conserve particle numbers by introducing individual (temperature-dependent) chemical potentials for each hadron. The final hadron spectra (dN/dp_T) are produced via a standard Cooper-Frye ansatz [34] at the kinetic freeze-out temperature ($T_{\text{fo}} = 120 \text{ MeV}$) when the hydrodynamical equations lose their validity, i.e. when the microscopic length (the hadrons mean free path) is no longer small compared to the size of the system. Unstable resonances are then allowed to decay with their appropriate branching ratios [35]. Table I summarizes the most important parameters describing our hydrodynamic evolution. The only free parameters are the initial energy density in the center of the reaction zone for head-on (impact parameter $b = 0$) Au+Au collisions, ε_0 , at the starting time, τ_0 , and the temperature at freeze-out time, T_{fo} .

Initialization. We distribute the initial energy density within the reaction volume according to the geometrical Glauber⁵ prescription proposed by Kolb *et al.* [37]. Such an ansatz ascribes 75% of the initial entropy production in a given centrality bin, $s_0(b)$, to soft processes (scaling with the transverse density of participant nucleons $N_{\text{part}}(b)$) and the remaining 25% to hard processes (scaling with the density of point-like collisions, $N_{\text{coll}}(b)$, proportional to the nuclear overlap function $T_{AA}(b)$). We then transform $\varepsilon_0(b) \propto s_0(b)^{4/3}$. This method provides a good description of the measured centrality dependence of the final hadron rapidity densities $dN/d\eta$ at RHIC [37,38]. For the initial conditions (Table 1), we choose $\varepsilon_0 = 220 \text{ GeV}/\text{fm}^3$ (maximum energy density at $b = 0 \text{ fm}$, corresponding to an *average* energy density over the total volume for head-on collisions of $\langle \varepsilon_0 \rangle = 72 \text{ GeV}/\text{fm}^3$) at a time $\tau_0 = 2R/\gamma \approx 0.15 \text{ fm}/c$ equal to the transit time of the two Au nuclei at $\sqrt{s_{\text{NN}}} = 200 \text{ GeV}$. The choice of this relatively short value of τ_0 , – otherwise typically considered in other hydrodynamical studies of thermal photon production at RHIC [10,14,39] –,

⁵ The density of participant and colliding nucleons are computed from $T_{AA}(b)$, parametrizing the Au nuclei with Woods-Saxon functions with radius $R = 6.38 \text{ fm}$ and diffusivity $a = 0.54 \text{ fm}$ [36].

rather than the standard thermalization time of $\tau_{therm} = 0.6 \text{ fm}/c$ [26–28], is driven by our will to consistently take into account within our space-time evolution the emission of photons from secondary “cascading” parton-parton collisions [40]. Such an emission takes place in the *thermalizing* phase, between prompt pQCD emission (at $\tau \sim 1/p_T \lesssim 0.15 \text{ fm}/c$) and full equilibration. Recent theoretical works [41,42] do support the application of hydrodynamics in such “pre-thermalization” conditions. Our consequent space-time evolution leads to a value of the energy density of $\varepsilon \approx 30 \text{ GeV}/\text{fm}^3$ at $\tau_{therm} = 0.6 \text{ fm}/c$, in perfect agreement with other 2D+1 hydrodynamic calculations [26,27] and more numerically involved 3D+1 approaches [28]. Thus, our calculations reproduce the final hadron spectra as well, at least, as those other works do⁶.

Table 1

Summary of the thermodynamical parameters characterizing our hydrodynamical model evolution for central ($b = 0 \text{ fm}$) Au+Au collisions at $\sqrt{s_{NN}} = 200 \text{ GeV}$. Input parameters are the (maximum) initial energy density ε_0 (with corresponding ideal-gas temperature T_0) at time τ_0 , and the chemical and kinetic freeze-out temperatures T_{chem} and T_{fo} (or energy density ε_{fo}). The energy densities at the end of the pure QGP (ε_{QGP}^{min}), and at the beginning of the pure hadron gas phase (ε_{HRG}^{max}) are also given, as well as the average (over total volume) values of the initial energy density $\langle \varepsilon_0 \rangle$ and temperature $\langle T_0 \rangle$.

| τ_0 (fm/c) | ε_0 ($\langle \varepsilon_0 \rangle$) (GeV/fm 3) | T_0 ($\langle T_0 \rangle$) (MeV) | ε_{QGP}^{min} (GeV/fm 3) | ε_{HRG}^{max} (GeV/fm 3) | T_{chem} (MeV) | T_{fo} (MeV) | $\varepsilon_{fo} = \varepsilon_{HRG}^{min}$ (GeV/fm 3) |
|--------------------|---|--|---|---|---------------------|-------------------|--|
| 0.15 | 220 (72) | 596 (378) | 1.7 | 0.35 | 150 | 120 | 0.10 |

Comparison to data. Figure 1 shows the pion, kaon, and proton⁷ transverse spectra measured by PHENIX [44], STAR [45,46], PHOBOS [47] and BRAHMS [31] in central (0–10% corresponding to $\langle b \rangle = 3.2 \text{ fm}$) and peripheral (60–70% corresponding to $\langle b \rangle = 11.9 \text{ fm}$) Au+Au collisions at $\sqrt{s_{NN}} = 200 \text{ GeV}$, compared to our hydrodynamical predictions (dashed lines) and to properly scaled p+p NLO pQCD expectations [48] (dotted lines). At low transverse momentum, the agreement data–hydro is excellent starting from the very low p_T PHOBOS data ($p_T < 100 \text{ MeV}$) up to at least $p_T \approx 1.5 \text{ GeV}/c$. Above this value, contributions from perturbative processes (parton fragmentation products) start to dominate over bulk hydrodynamic production. Indeed, particles with transverse momenta $p_T \gtrsim 2 \text{ GeV}/c$ are mostly produced in primary parton-parton collisions at times of order $\tau \sim 1/p_T \lesssim 0.15 \text{ fm}/c$ (i.e. during

⁶ As a matter of fact, by using $\tau_0 = 0.15 \text{ fm}/c$ (rather than $0.6 \text{ fm}/c$), the system has a few more tenths of fm/c to develop some extra transverse collective flow and there is no need to consider in our initial conditions a supplemental input radial flow velocity parameter, v_{r0} , [12,43] in order to reproduce the hadron spectra.

⁷ For a suitable comparison to the (feed-down corrected) PHENIX [44], PHOBOS [47] and BRAHMS [31] yields, the STAR proton spectra [45] have been appropriately corrected for a $\sim 40\%$ (p_T -independent) contribution from weak decays [46].

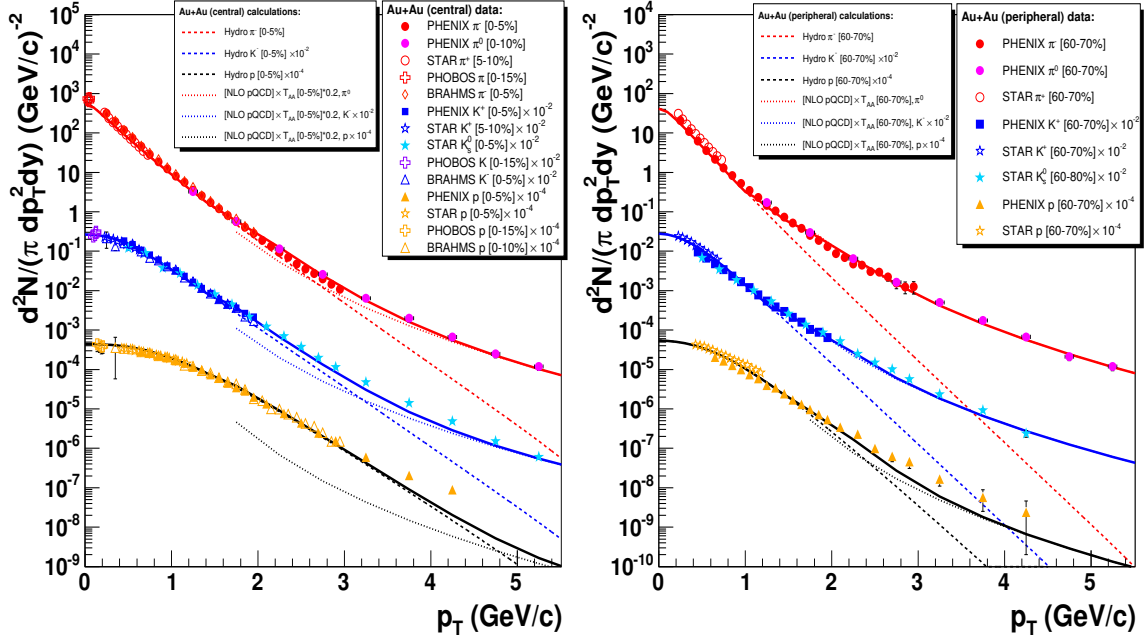


Fig. 1. Transverse momentum spectra for $\pi^{\pm,0}, K^{\pm,0}$, and protons measured in the range $p_T = 0 - 5.5$ GeV/c by PHENIX [44], STAR [45,46] (K_s^0 are preliminary), PHOBOS [47] and BRAHMS [31] in central (0-10% centrality, left) and peripheral (60-70%, right) Au+Au collisions at $\sqrt{s_{NN}} = 200$ GeV, compared to the theoretical expectations of hydrodynamics (dashed lines), scaled pQCD p+p rates [48] (dotted lines), and the sum hydro+pQCD (solid lines).

the interpenetration of the colliding nuclei and *before* any sensible time estimate for equilibration), and, as such, they are *not* in thermal equilibrium with the bulk particle production. Therefore, one does not expect hydrodynamics to reproduce the spectral shapes beyond $p_T \approx 2$ GeV/c (an exception to this behaviour being the heavier baryons at intermediate p_T 's, as discussed below). The dotted lines of Fig. 1 show NLO predictions for π , K and p production in p+p collisions at $\sqrt{s} = 200$ GeV [48] scaled by the number of point-like collisions ($N_{coll} \propto T_{AA}$) times an empirical quenching factor, $R_{AA} = 0.2$ (0.7) for 0-10% central (60-70% peripheral) Au+Au, to account for the observed constant suppression factor of hadron yields at high p_T [49,50]. It is clear from Fig. 1 that identified particle production at $y = 0$ in nucleus-nucleus collisions at RHIC is fully described in their whole p_T range and for all centralities by a combination of hydrodynamical (thermal+collective boosted) emission plus (quenched) prompt perturbative production. An exception to this rule are the protons [51]. Due to their higher masses, they get an extra push from the hydrodynamic flow up to $p_T \sim 3$ GeV/c. However, for higher transverse momenta the combination of hydro plus (quenched) pQCD clearly undershoots the experimental proton spectra lending support to the existence of an additional mechanism for baryon production at intermediate p_T values ($p_T \approx 3 - 5$ GeV/c) based on quark recombination [52]. This mechanism will not, however, be further considered in this paper since it has no practical implication

for photon production and/or the overall hydrodynamic evolution of the reaction. The good theoretical reproduction of the differential π, K, p experimental spectra ensures that the measured charged hadron multiplicity, $dN_{ch}/d\eta|_{\eta=0}$, is automatically well accounted for by our calculations. This observation is important for our later use of $dN_{ch}/d\eta|_{\eta=0}$ as an empirical quantity correlated with the initial entropy density (see Section 4).

3 Direct photon production

As in the case of hadron production, the total direct photon spectrum in a given Au+Au collision at impact parameter b is obtained by adding the primary production from perturbative parton-parton scatterings to the thermal emission rates integrated over the whole space-time volume of the produced fireball. Three sources of direct photons are considered corresponding to each one of the phases of the reaction: prompt production, partonic gas emission, and hadronic gas radiation. For the prompt γ production we use the NLO pQCD predictions of W. Vogelsang [53] scaled by the corresponding Glauber nuclear overlap function at b , $T_{AA}(b)$, as expected for hard processes in A+A collisions unaffected by medium effects (and empirically confirmed for photons [22]). This pQCD photon spectrum is obtained with CTEQ6M [54] parton distribution functions (PDF), GRV [55] parametrization of the $q, g \rightarrow \gamma$ fragmentation function (FF), and renormalization-factorization scales set equal to the transverse momentum of the photon ($\mu = p_T$). Such NLO calculations provide an excellent reproduction of the inclusive γ [23] (and high $p_T \pi^0$ [24]) spectra measured by PHENIX in p+p collisions at $\sqrt{s} = 200$ GeV without any additional parameter (in particular, at variance with results at lower energies [17], no primordial k_T is needed to describe the data). We do *not* consider any modification of the prompt photon yields in Au+Au collisions due to partially counteracting initial-state (IS) effects such as: (i) nuclear modifications (“shadowing”) of the Au PDF (< 20%, in the relevant (x, Q^2) kinematical range considered here [20,39,56]), and (ii) extra nuclear k_T broadening⁸ (Cronin enhancement) as described e.g. in [19]. Likewise, we do *not* take into account any possible final-state (FS) *photon* suppression due to energy loss of the jet-fragmentation (aka. “anomalous”) component of the prompt photon cross-section [19,56], which, if present at all (see discussion in [57]), can be in principle experimentally determined by detailed measurements of the isolated and non-isolated direct photon baseline spectra in p+p collisions at $\sqrt{s} = 200$ GeV [58].

⁸ The observed small Cronin effect for π^0 in d+Au at $\sqrt{s_{NN}} = 200$ GeV [25], $R_{dAu} \lesssim 1.2$, is *de facto* an upper limit for any Cronin enhancement for γ since, once produced, photons (at variance with partons fragmenting into π^0) do not suffer any multiple scattering in the medium.

For the QGP phase we use the most recent full leading order (in α_{em} and α_s couplings) emission rates from Arnold *et al.* [59]. These calculations include hard thermal loop diagrams to all orders and Landau-Migdal-Pomeranchuk (LPM) medium interference effects. The parametrization given in [59] assumes zero net baryon density (i.e. null quark chemical potential, $\mu_q = 0$), and *chemical* together with thermal equilibrium. Corrections of the QGP photon rates due to net quark densities are $\mathcal{O}[\mu_q^2/(\pi T)^2]$ [61] i.e. marginal at RHIC energies where the baryochemical potential is close to zero at midrapidity ($\mu_B = 3\mu_q \sim 25$ MeV) and neglected here. Similarly, although the early partonic phase is certainly not chemically equilibrated (the first instants of the reaction are strongly gluon-dominated) the two main effects from chemical non-equilibrium composition of the QGP: reduction of quark number and increase of the temperature, nearly cancel in the photon spectrum [7,60] and have not been considered either. For the HRG phase, we use the latest improved parametrization from Turbide *et al.* [62] which includes hadronic emission processes not accounted for in the literature before. In all calculations, we use a temperature-dependent parametrization of the strong coupling⁹, $\alpha_s(T) = 2.095/\{\frac{11}{2\pi} \ln(Q/\Lambda_{\overline{MS}}) + \frac{51}{22\pi} \ln[2 \ln(Q/\Lambda_{\overline{MS}})]\}$ with $Q = 2\pi T$, obtained from recent results in the lattice [63].

Apart from the aforementioned photon production mechanisms, S. Bass *et al.* [40] have recently evaluated within the Parton Cascade Model (PCM), the contribution to the total photon spectrum from secondary (cascading) parton-parton collisions taking place before the attainment of thermalization (i.e. between the transit time of the two nuclei, $\tau \approx 0.15$ fm/c, and the standard $\tau_{therm} = 0.6$ fm/c considered at RHIC). LPM interference effects are, however, absent in the PCM framework and the corresponding secondary rates are overestimated by up to a factor of ~ 4 , as the authors themselves acknowledge and the recent PHENIX data [22] indicate. Since such cascading light emission is due to second-chance partonic collisions which are, simultaneously, driving the system towards equilibrium, we consider not only “valid” (see the discussion of refs. [41,42]) but more realistic to consistently account for this contribution within our hydrodynamical evolution. We achieve that by starting hydrodynamics (whose photon rates do include the expected LPM reduction) at $\tau_0 = 0.15$ fm/c. By doing that, at the same time that we account for this second-chance emission, our initial plasma temperature and associated thermal photon production can be considered to be at their maximum values for RHIC energies. In a similar manner, we do not consider the conjectured extra γ emission due to the passage of quark jets (Compton-scattering and annihilating) through the medium [64] since the importance of this effect is probably overestimated in the calculations. Indeed, in their comparisons, Fries *et al.* [64] use a $K = 2.5$ factor to effectively account for the NLO jet(\rightarrow photon) cross-sections but use only LO yields (no K factor) for the “conventional” (perturbative and

⁹ According to this parametrization, $\alpha_S(T) = 0.3 - 0.6$ within $T \approx 600 - 150$ MeV.

thermal) γ cross-sections. Secondly, they do not quantitatively consider the concurrent non-Abelian energy loss suffered by the scattered quarks going through the medium [49,50], which will, at a given p_T , further comparatively reduce the jet–photon conversion rates.

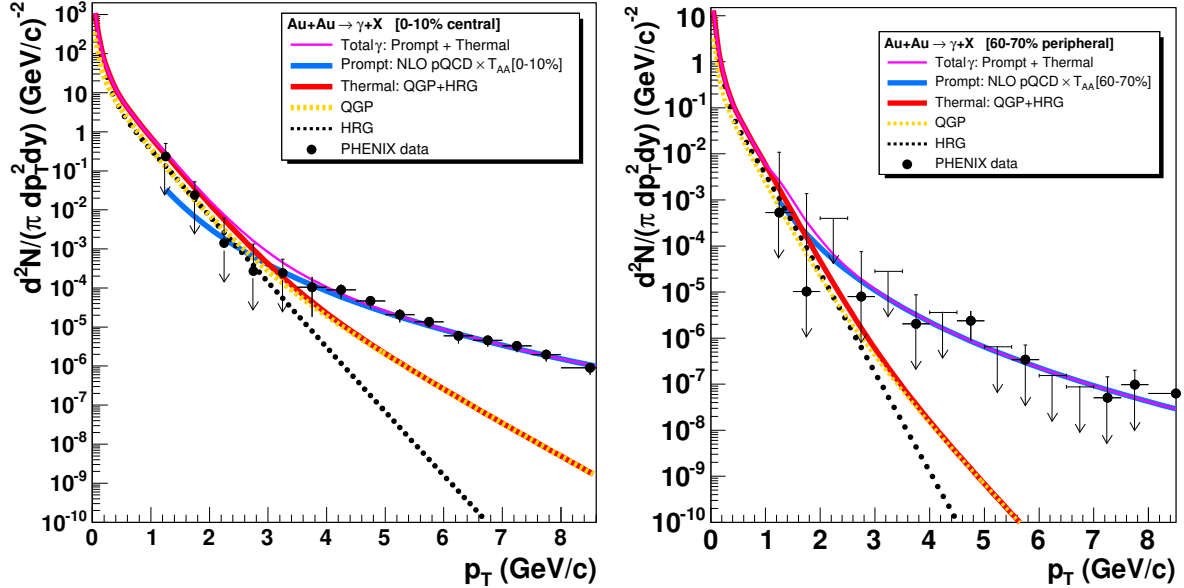


Fig. 2. Photon spectra for central (0–10%, left) and peripheral (60–70%, right) Au+Au reactions at $\sqrt{s_{NN}} = 200$ GeV as computed with our hydrodynamical model [with the contributions for the QGP and hadron resonance gas (HRG) given separately] compared to the expected NLO pQCD p+p yields for the prompt γ [53] (scaled by the corresponding nuclear overlap function), and to the experimental photon yields measured by the PHENIX collaboration [22].

Figure 2 shows our computed total photon spectra for central (left) and peripheral (right) Au+Au collisions at $\sqrt{s_{NN}} = 200$ GeV, with the pQCD, QGP, and HRG components differentiated¹⁰. In central reactions, thermal photon production (mainly of QGP origin) outshines the prompt pQCD emission below $p_T \approx 3$ GeV/c (within $p_T \approx 1 - 3$ GeV/c, thermal photons account for $\sim 90\% - 50\%$ of the total photon yield). Photon production in peripheral collisions is, however, completely dominated by the primary parton-parton radiation. In both cases, hadronic gas emission prevails only for lower p_T values. Such conclusions are also globally supported by previous hydrodynamical predictions for thermal photon yields in Au+Au collisions at top RHIC energy: N. Hammon *et al.* [39] (with initial conditions $\tau_0 = 0.12$ fm/c and $T_0 = 533$ MeV), Jan-e Alam *et al.* [11] ($\tau_0 = 0.5$ fm/c and $T_0 = 300$ MeV), D. K. Srivastava *et al.* [10] ($\tau_0 \approx 0.2$ fm/c and $T_0 \approx 450 - 660$ MeV), F. D. Steffen and M. H. Thoma [13] ($\tau_0 = 0.5$ fm/c and $T_0 = 300$ MeV), and S. S. Rasanen *et al.* [14] ($\tau_0 = 0.17$ fm/c and $T_0 = 580$ MeV). For similar initial conditions, the

¹⁰ We split the mixed phase contribution onto QGP and HRG components calculating the relative proportion of QGP (HRG) matter in it.

computed total thermal yields in those works are compatible within a factor of ~ 2 with those presented here. The agreement is specially good with the calculations of the Jyväskylä group [14] which have been computed with the same up-to-date QGP rate used here. More recently, thermal photon spectrum with the same emission rates used here have been also calculated by Turbide *et al.* [62] within a dynamical fireball model. Our QGP photon spectrum agrees very well with those calculations, but their hadron gas photon spectrum is significantly softer at high p_T . This discrepancy is not unexpected, however, since fireball models lack a selfconsistent treatment of the collective transverse expansion buildup which is known to strongly boost the particle spectra in full 2D(3D)+1 hydrodynamical calculations. In Figure 2 we also compare our computed spectra to the inclusive Au+Au photon spectra published recently by the PHENIX collaboration [22]. The total theoretical (pQCD+hydro) differential cross-sections are in good agreement with the experimental (upper limit) yields. Unfortunately, in the region of interest for the thermal photon signal ($p_T = 1 - 3$ GeV/c) the available data have still large uncertainties, precluding a more detailed data–model comparison at this point. Nonetheless, in the next section we provide indications of what kind of information can be obtained on the underlying degrees of freedom and on the thermodynamical properties of the produced QCD medium, by exploiting an identified thermal photon signal in Au+Au collisions at $\sqrt{s_{NN}} = 200$ GeV.

4 Thermal photons and the QCD equation-of-state

Experimentally, in order to extract the thermal photon signal one needs to subtract from the total γ spectrum the non-equilibrated “background” of prompt photons. The prompt γ contribution emitted in a given Au+Au centrality can be measured separately in reference p+p collisions at the same \sqrt{s} , scaled by the corresponding nuclear overlap function, and subtracted from the total Au+Au γ spectrum [58]. The expectation is that the remaining photon spectrum will be just that due to thermal emission from the partonic and hadronic phases of the reaction, and can be therefore subject to scrutiny in terms of the thermodynamical properties of the radiating medium. In a purely thermal system, the photon transverse momentum spectrum should be well described by an exponential distribution with inverse slope parameter proportional to the system temperature. This naive assumption is, however, complicated by the fact that, as seen in the previous sections, different p_T ranges of the photon spectrum are dominated by emission from phases with different temperatures and, collective flow effects enhance the purely thermal emission leading to an effectively larger inverse slope parameter ($T_{\text{eff}} \approx \sqrt{(1 + \beta)/(1 - \beta) T}$) [12]. To assess to what extent the thermal slopes are indicative of the original temperature of the system, we have fitted the thermal spectra obtained from our

hydrodynamical calculations in different Au+Au centralities (corresponding to different maximal initial temperatures T_0) to an exponential distribution in different p_T ranges. The upper plot of Figure 3 shows the obtained local slope parameter, T_{eff} , as a function of the initial (maximum) temperature, T_0 for the default QGP+HRG hydrodynamical evolution. The photon slopes are indeed approximately proportional to the system temperature. The higher the p_T range, the closer is T_{eff} to the original T_0 . According to our calculations, empirical thermal slopes above $p_T \approx 4$ GeV/c in central Au+Au collisions are above ~ 400 MeV i.e. only $\sim 30\%$ lower than the “true” maximal (local) temperature of the quark-gluon phase. On the other hand, local γ slopes below $p_T \approx 1$ GeV/c have a constant value $T_{\text{eff}} \sim 200$ MeV (numerically close to T_{crit}) and are almost insensitive to the initial temperature of the hydrodynamical system but mainly specified by exponential prefactors in the hadronic emission rates.

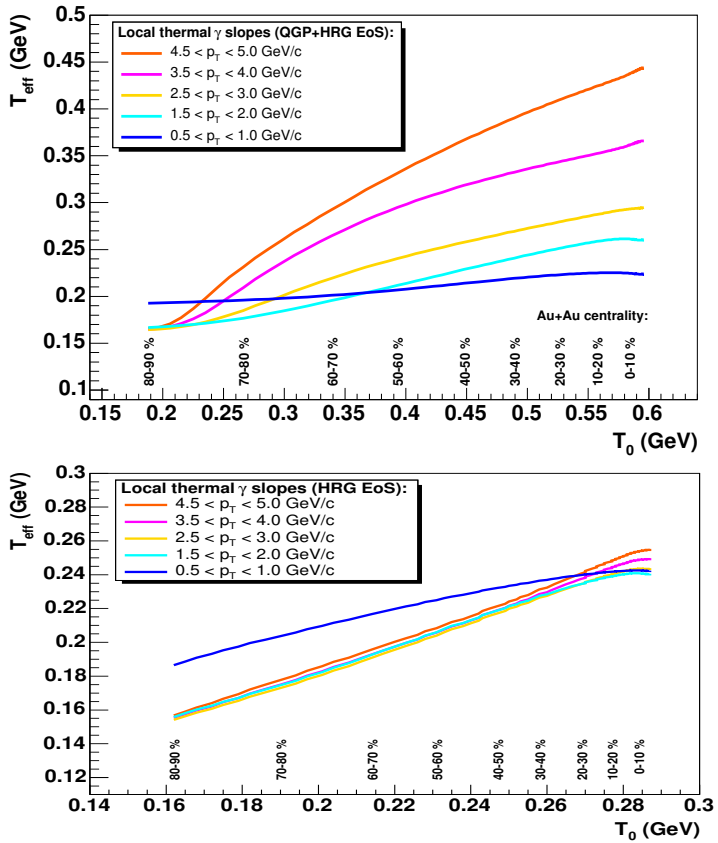


Fig. 3. Local photon slope parameters, T_{eff} , (obtained from exponential fits of the thermal photon spectrum in different p_T ranges) plotted versus the initial (maximum) temperature, T_0 , of the fireball produced in Au+Au collisions at $\sqrt{s} = 200$ GeV at different centralities. Upper plot - hydrodynamical calculations with QGP+HRG EoS (Table 1), bottom - HRG EoS (with initial conditions: $\varepsilon_0 = 30$ GeV/fm 3 at $\tau_0 = 0.6$ fm/c).

To assess the photon spectral shapes in a hydrodynamical evolution *without* the formation of a weakly interacting QGP, we have rerun our hydro evolution

just with the EoS of a hadron resonance gas starting with $\varepsilon_0 = 30 \text{ GeV}/\text{fm}^3$ at $\tau_0 = 0.6 \text{ fm}/c$, which can still reasonably describe the experimental hadron spectra. Obviously, any description in terms of hadronic degrees of freedom at such high initial energy densities is unrealistic but we are interested in assessing the effect on the photon spectra of a non-ideal EoS incorporating large number of heavy resonances (more generally, of any EoS with exponentially rising number of mass states). The photon slopes for the pure HRG gas EoS (Fig. 3, bottom) are lower ($T_{\text{eff}}^{\text{max}} \approx 220 \text{ MeV}$) than in the default QGP+HRG evolution, not only because the input HRG ε_0 is smaller (the evolution starts at a later τ_0) but, specially because for the same initial ε_0 the effective number of degrees of freedom in a HRG is higher than in a QGP (see later) and therefore the initial temperatures are lower. A second difference is that, for all p_T ranges, we find almost the same exact correlation between the local γ slope and T_0 indicating a single underlying (hadronic) radiation mechanism dominating the transverse spectra at all p_T . Two overall conclusions can be obtained from the study of the hydrodynamical photon slopes. First, the observation in the data of a thermal photon component above $p_T \approx 2.5 \text{ GeV}/c$ with exponential slope $T_{\text{eff}} \gtrsim 250 \text{ MeV}$ is an unequivocal proof of the formation of a system with maximum temperatures above T_{crit} since no realistic collective flow mechanism can generate such a strong boost of the photon slopes, while simultaneously reproducing the hadron spectra. Secondly, pronounced p_T and centrality dependences of the thermal slopes can only be reproduced by space-time evolutions of the reaction that include an ideal QGP radiating phase.

One can go one step further beyond the mere analysis of the thermal photon slopes and try to get a more direct handle on the equation of state of the radiating medium by looking at the correlation of T_{eff} with observables related to the initial energy or entropy densities of the system. Indeed, the most clear evidence of QGP formation from QCD calculations on the lattice is the sharp rise of $\varepsilon(T)/T^4$ or, equivalently, of $s(T)/T^3$ at temperatures around T_{crit} . This sharp jump is of course due to the sudden release of a large number of (partonic) degrees of freedom at T_{crit} . From the entropy density¹¹, s , and temperature, T , of the system we can define the effective number of degrees of freedom via the relation¹²

$$g(s, T) = \frac{\pi^2}{4} \zeta(4) \frac{s}{T^3} (\hbar c)^3 = \frac{45}{2\pi^2} \frac{s}{T^3} (\hbar c)^3, \quad (1)$$

¹¹ We use the entropy- rather than the energy-density to determine g_{eff} since $dN/dy(\propto s_0)$ remains constant in an isentropic expansion whereas, due to longitudinal work, the final dE_T/dy provides only a lower limit on ε_0 . Additionally, $g_{\text{eff}} \propto s/T^3$ is less sensitive to uncertainties in the measurement of T than $g_{\text{eff}} \propto \varepsilon/T^4$.

¹² Units are in GeV and fm. $\zeta(4) = \pi^2/90$, where $\zeta(n)$ is the Riemann zeta function.

which coincides with the degeneracy of a weakly interacting gas of massless particles. The dashed line in Fig. 4 (top) shows the evolution of the “true” number of degrees of freedom, $g_{hydro}(s_0, T_0)$, computed via Eq. (1), as a function of the initial (maximal) temperatures and entropies of the system (corresponding to different Au+Au centralities at 200 GeV) directly from the EoS implemented in our hydrodynamical model¹³. Note that it remains constant at the expected degeneracy, $g_{hydro} = 42.25$, of an ideal gas of $N_f = 2.5$ quarks and gluons for basically *all* the maximum temperatures accessible in the different centralities of Au+Au at $\sqrt{s_{NN}} = 200$ GeV¹⁴.

We can empirically trace the QCD EoS shown in Fig. 4 (and eventually determine the evolution of the degeneracy of the produced medium) using the estimate of the initial temperature given by the thermal photon slopes, T_{eff} , and a second observable closely related to the initial entropy of the system such as the final-state hadron multiplicity, dN/dy . Indeed, in the absence of dissipative effects, the space-time evolution of the produced system in a nucleus-nucleus reaction is isentropic and the initial entropy density (per unit rapidity) can be directly connected (via $s = 4\zeta(4)/\zeta(3)\rho \approx 3.6\rho$) to the final charged hadron pseudo-rapidity density¹⁵:

$$s \approx 3.6 \cdot \frac{dN}{dV} \approx \frac{4.3}{\langle A_{\perp} \rangle \cdot \tau_0} \cdot \frac{dN_{ch}}{d\eta}. \quad (2)$$

where we have written the volume, $dV = \langle A_{\perp} \rangle \tau_0 d\eta$, as the product of the (Glauber) average transverse overlap area times the starting proper time of our hydro evolution ($\tau_0 = 0.15$ fm/c), and where $dN_{ch}/d\eta$ is the *charged* hadron multiplicity customarily measured experimentally at mid-rapidity. By combining, Eqs. (1) and (2), we obtain the following estimate for the initial degrees of freedom of the system produced in a given A+A collision (with experimentally measured $dN_{ch}/d\eta$ and inverse thermal photon slope T_{eff}) at impact parameter b :

$$g_{eff}(dN_{ch}/d\eta(b), T_{eff}(b)) = \frac{100}{\pi^2} \frac{dN_{ch}/d\eta(b)}{\langle A_{\perp}(b) \rangle \cdot \tau_0 \cdot T_{eff}^3(b)} (\hbar c)^3, \quad (3)$$

Such an estimate provides indeed a direct experimental handle on the form

¹³ The bag entropy has been subtracted to make more apparent the drop near T_c .

¹⁴ At top RHIC energies and for most of centralities, T_0 is (well) above T_{crit} and the hottest parts of the fireball are in the QGP phase. The expected drop in g_{hydro} related to the transition to the hadronic phase is only seen for the very most peripheral reactions (with $T_0 \approx T_c$). Thus, probing the QGP-HRG phase change itself by studying the centrality dependence of experimental observables would only be potentially feasible in Au+Au reactions at *lower* center-of-mass energies [38].

¹⁵ We have used: $N_{tot}/N_{ch} = 3/2$, and $|d\eta/dy| \approx 0.8$.

of the underlying EoS as shown by the dotted-dashed line in Fig. 4 obtained using the $dN_{ch}/d\eta$ from our hydrodynamical model, and the “true” initial temperature of the system, T_0 . Eq. (3) underestimates by a factor of ~ 6 the maximal entropy of the original medium, i.e. $g_{eff}(dN_{ch}/d\eta, T_0) \approx 6 \cdot g_{hydro}(s_0, T_0)$, because $dN_{ch}/d\eta / \langle A_T \rangle$ specifies the entropy integrated over transverse area which is ~ 6 times smaller than the maximal value corresponding to T_0 in the center of the collision region. Thus, although Eq. (3) does not provide the true *absolute* number of degrees of freedom, it does provide a very reliable indication of the dependence of g_{eff} on the temperature of the system and, therefore, of the exact form of the underlying EoS. The different solid curves in the upper plot of Fig. 4 show the effective degeneracy, g_{eff} , computed using Eq. (3) and the local photon slopes T_{eff} measured in different p_T ranges for our default QGP+HRG evolution. As one could expect from Fig. 3, the best reproduction of the shape of the underlying EoS (dashed-dotted curve) is obtained with the effective temperatures measured in higher p_T bins. For those T_{eff} , the computed g_{eff} show a relatively constant value in a wide range of centralities as expected for a weakly interacting QGP. Deviations from this ideal-gas plateau appear for more central collisions, due to an increasing difference between the (high) initial temperatures, T_0 , and the apparent temperature given by the photon slopes (Fig. 3). Such deviations do not spoil the usefulness of our estimate however, since, a non ideal-QGP EoS would result in a considerably different dependence of g_{eff} on the reaction centrality. Indeed, the different curves in the bottom plot of Fig. 4 obtained with a pure hadron resonance gas EoS clearly indicate¹⁶ that any EoS with exponentially increasing number of mass states would bring about a much more dramatic rise of g_{eff} with T_{eff} .

5 Conclusions

We have studied thermal photon production in Au+Au reactions at $\sqrt{s_{NN}} = 200$ GeV using a 2D+1 hydrodynamic model with longitudinal boost invariance. We choose the initial conditions of the hydrodynamical evolution so as to efficiently reproduce the identified hadron spectra measured in Au+Au at all centralities at RHIC. The obtained direct photon spectra, combined with the pQCD prompt γ , are in good agreement with the Au+Au direct photon (upper limit) yields measured by the PHENIX experiment. In central collisions, a thermal photon signal should be identifiable as a factor of $\sim 1 - 5$ excess over the perturbative γ component within $p_T \approx 1 - 3$ GeV/c, whereas pure prompt (pQCD) gamma emission clearly dominates the photon spectra at all p_T in peripheral reactions. The inverse slope parameter of the thermal

¹⁶ Accidentally, $g_{eff} \approx g_{hydro}$ in the case of a HRG EoS, because the underestimation of the apparent temperature (raised to the cube) compensates for the aforementioned volume “overnormalization” of the entropy.

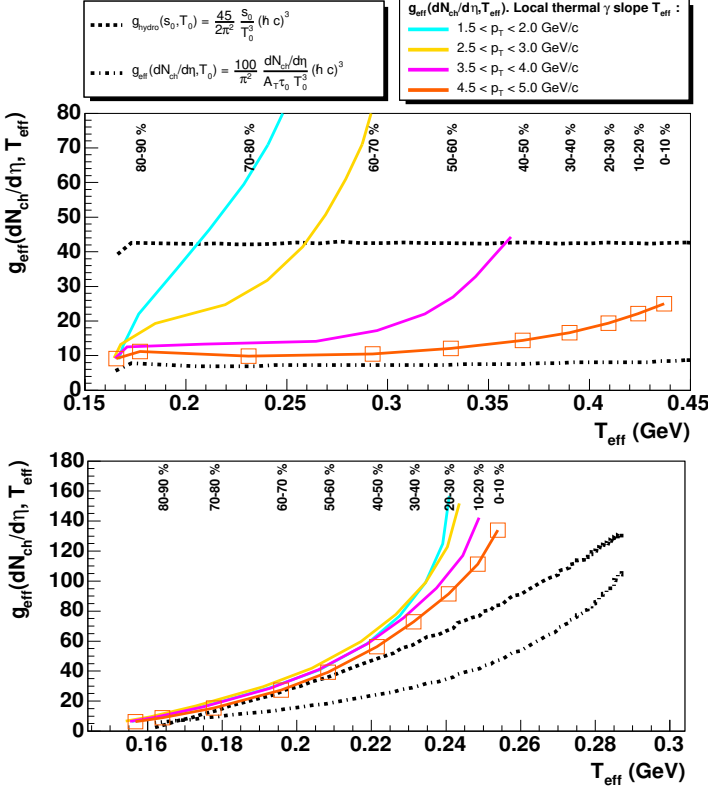


Fig. 4. Effective initial number of degrees of freedom obtained from our hydrodynamical calculations with a QGP+HRG EoS (upper plot), and with a pure HRG EoS (bottom), plotted as a function of the thermal photon slope (T_{eff}) in different Au+Au centrality classes at $\sqrt{s_{NN}} = 200$ GeV. The number of degrees of freedom are computed respectively: (i) From our initial thermodynamical conditions (s_0, T_0), via Eq. (1) (dashed line), (ii) from the obtained charged hadron multiplicity, $dN_{ch}/d\eta$, and the *true* initial temperature T_0 , via Eq. (3) (dotted-dashed line); and (iii) from $dN_{ch}/d\eta$ and the thermal photon slopes, T_{eff} , measured in different p_T ranges, via Eq. (3) (solid lines). For illustrative purposes, we indicate the approximate position of the different Au+Au centrality classes for the values of g_{eff} obtained using the thermal photon slopes measured above $p_T = 4$ GeV/c.

photon spectrum is directly correlated to the maximum temperature attained in the collision. The experimental measurement of local thermal photon slopes above $p_T \approx 2.5$ GeV/c, with values $T_{\text{eff}} \gtrsim 250$ MeV and with pronounced p_T and centrality dependences can only be reproduced by space-time evolutions of the reaction that include an ideal QGP phase. Finally, we have proposed and tested an empirical method to determine the effective number of degrees of freedom of the produced medium by correlating the thermal photon slopes with the final-state charged hadron multiplicity measured in different centrality classes. We found that one can clearly distinguish between the equation of state of a weakly interacting quark-gluon plasma and that of a system with rapidly rising number of mass states with T . The requirement for hydrodynamical models of concurrently describing the experimental bulk hadron and

thermal photon spectra for different Au+Au centralities at $\sqrt{s_{NN}} = 200$ GeV, imposes very strict constraints on the form of the equation of state of the underlying expanding matter produced in the reaction.

6 Acknowledgments

We would like to thank Werner Vogelsang for providing us with his NLO pQCD calculations for photon production in p+p collisions at $\sqrt{s} = 200$ GeV; Sami Rasanen for valuable comments on hydrodynamical photon production; and Helen Caines and Olga Barannikova for useful discussions on (preliminary) STAR hadron data. D.P. acknowledges support from MPN of Russian Federation under grant NS-1885.2003.2.

References

- [1] See e.g. F. Karsch, *Lect. Notes Phys.* **583**, 209 (2002).
- [2] U.W. Heinz and M. Jacob, nucl-th/0002042.
- [3] M. Gyulassy and L. McLerran, *Nucl. Phys. A* **750** (2005)30; nucl-th/0405013.
- [4] E. L. Feinberg, *Nuovo Cim. A* **34** (1976) 391.
- [5] E. V. Shuryak, *Phys. Lett. B* **78** (1978) 150 [Sov. J. Nucl. Phys. **28** (1978) YAFIA,28,796-808.1978] 408.1978 YAFIA,28,796].
- [6] T. Peitzmann and M. H. Thoma, *Phys. Rept.* **364** (2002) 175.
- [7] F. Arleo *et al.*, in CERN Yellow Report on Hard Probes in Heavy Ion Collisions at the LHC; hep-ph/0311131.
- [8] C. Gale and K. L. Haglin, in “Quark Gluon Plasma. Vol 3” Eds: R.C. Hwa and X.N. Wang, World Scientific, Singapore; hep-ph/0306098.
- [9] M. M. Aggarwal *et al.*, WA98 Collaboration, *Phys. Rev. Lett.* **85** (2000) 3595.
- [10] D. K. Srivastava and B. Sinha, *Phys. Rev. C* **64** (2001) 034902; D. K. Srivastava, *Pramana* **57** (2001) 235.
- [11] J. e. Alam, S. Sarkar, T. Hatsuda, T. K. Nayak and B. Sinha, *Phys. Rev. C* **63** (2001) 021901.
- [12] D. Y. Peressounko and Y. E. Pokrovsky, *Nucl. Phys. A* **624** (1997) 738, hep-ph/9704386; *Nucl. Phys. A* **669** (2000) 196, hep-ph/9906325; hep-ph/0009025.
- [13] F. D. Steffen and M. H. Thoma, *Phys. Lett. B* **510** (2001) 98.

- [14] P. Huovinen, P. V. Ruuskanen and S. S. Rasanen, *Phys. Lett. B* **535** (2002) 109; S. S. Rasanen, *Nucl. Phys. A* **715** (2003) 717; H. Niemi, S. S. Rasanen and P.V. Ruuskanen in [7].
- [15] D. d'Enterria, *Phys. Lett. B* **596** (2004) 32, nucl-ex/0403055.
- [16] L. Apanasevich *et al.*, *Phys. Rev. D* **63** (2001) 014009.
- [17] C. Y. Wong and H. Wang, *Phys. Rev. C* **58** (1998) 376.
- [18] J.W. Cronin *et al.*, *Phys. Rev. D* **11**, 3105 (1975); D. Antreasyan *et al.*, *Phys. Rev. D* **19** 764, (1979).
- [19] A. Dumitru and N. Hammon, hep-ph/9807260; A. Dumitru, L. Frankfurt, L. Gerland, H. Stocker and M. Strikman, *Phys. Rev. C* **64** (2001) 054909.
- [20] S. Jeon, J. Jalilian-Marian and I. Sarcevic, *Nucl. Phys. A* **715** (2003) 795.
- [21] G. Papp, G. I. Fai and P. Levai, hep-ph/9904503.
- [22] J. Frantz, PHENIX Collaboration, *J. Phys. G*, **30** (2004) S1003, nucl-ex/0404006; S.S. Adler *et al.*, PHENIX Collaboration, nucl-ex/0503003.
- [23] K. Okada, PHENIX Collaboration *Proceeds. SPIN'04*, hep-ex/0501066; S.S. Adler *et al.*, PHENIX Collaboration, hep-ex/0502006.
- [24] S.S. Adler *et al.*, PHENIX Collaboration, *Phys. Rev. Lett.* **91**, 241803 (2003).
- [25] S. S. Adler *et al.*, PHENIX Collaboration, *Phys. Rev. Lett.* **91** (2003) 072303; H. Busching, PHENIX Collaboration, nucl-ex/0410002.
- [26] P. F. Kolb and U. Heinz, in “Quark Gluon Plasma. Vol 3” Eds: R.C. Hwa and X.N. Wang, World Scientific, Singapore; nucl-th/0305084, and refs. therein.
- [27] D. Teaney, J. Lauret and E. V. Shuryak, nucl-th/0110037.
- [28] T. Hirano and K. Tsuda, *Phys. Rev. C* **66** (2002) 054905, T. Hirano and Y. Nara, *Phys. Rev. C* **69** (2004) 034908, nucl-th/0307015.
- [29] B. Mohanty and J. e. Alam, *Phys. Rev. C* **68** (2003) 064903.
- [30] J. D. Bjorken, *Phys. Rev. D* **27** (1983) 140.
- [31] I. G. Bearden *et al.*, BRAHMS Collaboration, nucl-ex/0403050; I. Arsene *et al.*, BRAHMS Collaboration, nucl-ex/0503010.
- [32] K. J. Eskola, K. Kajantie and P. V. Ruuskanen, *Eur. Phys. J. C* **1** (1998) 627.
- [33] P. Braun-Munzinger, K. Redlich and J. Stachel, in “Quark Gluon Plasma. Vol 3” Eds: R.C. Hwa and X.N. Wang, World Scientific, Singapore, nucl-th/0304013.
- [34] F. Cooper and G. Frye, *Phys. Rev. D* **10** (1974) 186.
- [35] K. Hagiwara *et al.* , Particle Data Group Collaboration, *Phys. Rev. D* **66** (2002) 010001.

- [36] B. Hahn, D.G. Ravenhall and R. Hofstadter, Phys. Rev. **101**, (1956) 1131,
- [37] P. F. Kolb, U. W. Heinz, P. Huovinen, K. J. Eskola and K. Tuominen, Nucl. Phys. A **696** (2001) 197
- [38] D. d'Enterria and D. Peressounko, in preparation.
- [39] N. Hammon, A. Dumitru, H. Stoecker and W. Greiner, Phys. Rev. C **57** (1998) 3292.
- [40] S. A. Bass, B. Muller and D. K. Srivastava, Phys. Rev. Lett. **90** (2003) 082301.
- [41] J. Berges, S. Borsanyi and C. Wetterich, Phys. Rev. Lett. **93** (2004) 142002.
- [42] P. Arnold, J. Lenaghan, G. D. Moore and L. G. Yaffe, nucl-th/0409068.
- [43] P. F. Kolb and R. Rapp, Phys. Rev. C **67** (2003) 044903.
- [44] S. S. Adler *et al.* , PHENIX Collaboration, Phys. Rev. C **69** (2004) 034909, nucl-ex/0307022.
- [45] J. Adams *et al.*, STAR Collaboration, Phys. Rev. Lett. **92** (2004) 112301, nucl-ex/0310004.
- [46] H. Caines, nucl-ex/0412016; O. Barannikova, STAR Collaboration, nucl-ex/0408022 and private communication.
- [47] B.B. Back *et al.*, PHOBOS Collaboration, nucl-ex/0401006.
- [48] F. Aversa *et al.* Nucl. Phys. B **327** (1989) 105; B. Jager *et al.* Phys. Rev. D **67** (2003) 054005; W. Vogelsang, private communication (NLO spectra have been computed with CTEQ6 PDFs, KKP FFs, and scales set to the hadron p_T).
- [49] S. S. Adler *et al.*, PHENIX Collaboration Phys. Rev. Lett. **91** (2003) 072301.
- [50] J. Adams *et al.*, STAR Collaboration, Phys. Rev. Lett. **91** (2003) 172302
- [51] K. Adcox *et al.*, PHENIX Collaboration, Phys. Rev. Lett. **88** (2002) 242301, nucl-ex/0112006; S. S. Adler *et al.* , PHENIX Collaboration, Phys. Rev. Lett. **91** (2003) 172301, nucl-ex/0305036.
- [52] R. J. Fries, J. Phys. G **30** (2004) S853, nucl-th/0403036, and refs. therein.
- [53] L.E. Gordon and W. Vogelsang, Phys. Rev. D **48** (1993) 3136; Phys. Rev. D **50** (1994) 1901, and W. Vogelsang (private communication).
- [54] S. Kretzer, H. L. Lai, F. I. Olness and W. K. Tung, Phys. Rev. D **69**, 114005 (2004).
- [55] M. Gluck, E. Reya and A. Vogt, Phys. Rev. D **48** (1993) 116 [Erratum-ibid. D **51** (1995) 1427].
- [56] J. Jalilian-Marian, K. Orginos and I. Sarcevic, Phys. Rev. C **63** (2001) 041901.
- [57] B. G. Zakharov, JETP Lett. **80** (2004) 1 [Pisma Zh. Eksp. Teor. Fiz. **80** (2004) 3].

- [58] D. d'Enterria, *J. Phys. G*, **31** (2005) S491.
- [59] P. Arnold, G. D. Moore and L. G. Yaffe, JHEP **0112** (2001) 009.
- [60] F. Gelis, H. Niemi, P. V. Ruuskanen and S. S. Rasanen, J. Phys. G **30** (2004) S1031, nucl-th/0403040.
- [61] C. T. Traxler, H. Vija and M. H. Thoma, Phys. Lett. B **346** (1995) 329, hep-ph/9410309.
- [62] S. Turbide, R. Rapp and C. Gale, Phys. Rev. C **69** (2004) 014903.
- [63] O. Kaczmarek, F. Karsch, F. Zantow and P. Petreczky, Phys. Rev. D **70** (2004) 074505.
- [64] R. J. Fries, B. Muller and D. K. Srivastava, Phys. Rev. Lett. **90** (2003) 132301.